A missense mutation in the *acnB* gene indirectly affects the growth, metabolism and biological fitness in a spontaneous compensatory mutant of antibiotic-resistant *Neisseria gonorrhoeae*

Samuel Kerr

Lab of Dr. Robert Nicholas

Abstract

Neisseria gonorrhoeae, the causative agent of the sexually transmitted infection gonorrhea, has developed resistance to every antimicrobial used against it. Ceftriaxone-resistant *N. gonorrhoeae* strains harbor mosaic *penA* alleles that encode highly mutated forms of Penicillin-Binding Protein 2 (PBP2), the lethal target of ceftriaxone. When bacteria develop resistance to antibiotics through an extensive alteration of an essential protein, they often incur a fitness cost. To have success as a pathogen, they must overcome this fitness deficit. We have hypothesized that antibiotic-resistant clinical isolates acquire compensatory mutations to help alleviate the fitness cost associated with resistance. Wild-type strains harboring a mosaic *penA* allele have reduced fitness both *in vitro* and *in vivo*, but compensatory mutants with increased biological fitness were isolated. In one such strain, a mutation (G348D) in *acnB*, which encodes the tricarboxylic acid (TCA) cycle aconitase, was identified. The hallmark of this compensatory mutant is that it grows rapidly during log-phase growth, but then plateaus early as it enters into stationary phase growth. The *acnB*-G348D mutation is both necessary and sufficient to impart the growth phenotype characteristic of compensatory mutant. Western blots of AcnB during the growth cycle show that wild-type AcnB increases in abundance as the cells enter stationary phase, whereas in the AcnB mutant, expression decreases by 2- to 3- fold. Interestingly, *acnB* mRNA levels do not account for changes in AcnB protein levels. These data suggest that *acnB*-G348D acts as a functional knockout in regards to the role of AcnB in the TCA cycle. Any fitness benefits associated with this mutation do not appear to be directly associated with the activity of AcnB in the TCA cycle.

Introduction

Neisseria gonorrhoeae, the causative agent of the sexually transmitted infection gonorrhea, is the second most common STI in the United States, with 350,062 cases reported by the CDC in 2014 (an increase of 10.5% since 2010). Since *N. gonorrhoeae* infections are often asymptomatic in women, they can go untreated, leading to further dissemination of the infection and to a variety of sequelae, including pelvic inflammatory disease (PID) and ectopic pregnancy. There is also evidence that a gonococcal infection can increase the risk of both acquiring and transmitting HIV [1] [2]. Unfortunately, *N. gonorrhoeae* has become resistant to essentially all antibiotics used to treat infections. The emergence of fluoroquinolone-resistant strains in the United States in 2007 caused the CDC to remove fluorquinolones from treatment guidelines, leaving only ceftriaxone and cefixime, and in 2010 the CDC removed cefixime from the list of recommended antibiotics. In 2015, the guidelines were changed to a dual therapy of ceftriaxone and azithromycin. Worryingly, multiple strains with high-level resistance to either ceftriaxone or azithromycin were identified internationally during that period [3].

Ceftriaxone-resistant isolates have been shown to contain mosaic *penA* alleles encoding a highly mutated Penicillin-Binding Protein 2 (PBP2). PBP2 is an essential peptidoglycan transpeptidase during cell wall synthesis in bacteria and is the lethal target of β-lactam antibiotics such as ceftriaxone and penicillin [4]. Although the mutations in the mosaic *penA* alleles contribute to increased resistance, they also confer a biological fitness cost thought to be due to the reduced peptidoglycan transpeptidase activity of PBP2 caused by the mutations. Preliminary experiments using the female model of infection have shown that a wild-type gonococcal strain, FA19, carrying the mosaic *penA41* allele from the ceftriaxone-resistant strain H041 also have a significant biological fitness deficit. Our collaborators in the Jerse lab had previously shown that *N. gonorrhoeae* can acquire spontaneous compensatory mutations in the host to overcome the biological fitness cost of fluoroquinolone-resistant alleles [5]. Consistent

with this, several isolates of FA19 *penA41* harboring compensatory mutations were isolated from infected mice that increased fitness without decreasing resistance. One of these strains, LV41C, contained a point mutation the *acnB* gene (coding for the TCA cycle enzyme, aconitase) causing an amino acid change from a glycine to aspartic acid at position 348. My research project was focused investigating the mechanisms by which this mutation helps compensate for the biological fitness deficit caused by the *penA41* allele.

In many species, the cost of carrying a resistance allele is associated with an increased metabolic stress, either directly through increased transcription, translation, and/or DNA replication, or more indirectly through an induction of altered physiology and metabolism of the bacterium. *In vitro* experiments with amoxicillin-resistant strains of *E. coli* showed that upon initial acquisition of the resistance allele, the strains had an increased metabolic cost when compared to the parental strain; however, subsequent generations experienced a decreased metabolic cost when compared to the initial resistant strain [6]. Other studies have shown that the exact cost of a resistance allele is extremely variable and dependent on the specific species and genotype [7]. It is important to note that the mechanisms used to overcome fitness costs *in vitro* may result in a decreased fitness *in vivo* because the metabolic environment is often very different *in vitro* than *in vivo* [8]. With clinical isolates of drug-resistant *Mycobacterium tuberculosis*, it was observed that only strains with a relatively high fitness were isolated, and fitness may determine the future evolution of multidrug-resistant strains [9].

Metabolism in *N. gonorrhoeae* is very streamlined and suited to conditions *in vivo*. The vaginal tract is the primary site of gonococcal infections and the two main carbon sources present in the vaginal cavity are glucose and lactate (as lactic acid). Although the amount of free glucose is limited, glycogen is readily supplied by the vaginal epithelia and subsequently broken down by resident flora or enzymes present in the vaginal tract into free glucose, or further degraded by the vaginal flora into lactic acid [3] [10]. *N. gonorrhoeae* can effectively utilize only glucose, lactate, or pyruvate as a carbon source [11], but pyruvate does not appear to be

biologically relevant. The gonococcus also has a variety of unusual alterations in metabolism, namely a non-functional TCA cycle during active growth on glucose [12]. Aconitase and isocitrate dehydrogenase, most classically defined as “essential” enzymes for aerobic organisms, are inactive during active growth in glucose, and the gonococcus instead uses glutamate and the enzyme PEP carboxylase to generate α-ketoglutarate and oxaloacetate, respectively [12]. In other species, such as *E. coli*, the presence of large quantities of glucose can repress the TCA cycle in order to streamline metabolism [13]. The adaptation of *N. gonorrhoeae* to such a glucose-rich environment may explain why the TCA cycle is downregulated. Paradoxically, despite not having a functional TCA cycle during active growth on glucose, the gonococcus utilizes the Entner-Doudoroff pathway for glycolysis, which is half as efficient as the Embden-Meyerhof-Parnas pathway as it only generates 1 net ATP and 1 net reduced pyridine nucleotide per molecule of glucose [11]. Other unusual alterations in metabolism include pyridine nucleotide-independent lactic acid dehydrogenases, which may help with lactate acquisition, and a NAD^+/$NADP^+$ non-specific glucose-6-phosphate dehydrogenase [14] [12].

Here we present evidence demonstrating that wild-type strains carrying the *penA41* allele from the ceftriaxone-resistant strain H041 have a significant biological fitness deficit. We have also demonstrated that strains can overcome this deficit by acquiring spontaneous compensatory mutations. One of the mutants identified contained a mutation (*acnB*-G348D) in the gene encoding the TCA cycle enzyme aconitase. Because antibiotic resistance alleles can impose a biological fitness deficit through the form of an increased metabolic stress and this compensatory mutation is in a metabolism gene, we have reason to suspect that this mutation may be altering the metabolism of *N. gonorrhoeae* either directly or indirectly, and ameliorating the metabolic stress on the organism. My project focused on elucidating the mechanism(s) by which this mutation overcomes the fitness deficit associated with carrying the *penA41* allele.

Methods

1. Media

N. gonorrhoeae strains were grown in liquid GCB media or on GCB agar plates at 37°C with Supplements I (glucose, glutamine, and cocarboxylase) and II (12 μM $Fe(NO_3)_3$) [15]. Agar plates were grown under 4% CO_2 whereas liquid media was supplemented with 10 mM $NaHCO_3$. Media containing lactate as the carbon source instead of glucose was made by substituting sodium lactate at a 1:1 molar ratio for glucose in Supplement I at pH 7.0. *E. coli* strains were grown in liquid LB media or on LB agar plates at 37 °C.

2. Growth Curves

N. gonorrhoeae strains were streaked from frozen stocks onto GCB agar plates containing the appropriate carbon source and incubated overnight at 37°C in a humidified 4% CO_2 incubator. Non-piliated colonies were selected, plated and the bacteria were swabbed after 17h of growth and used to inoculate liquid GCB media to give a starting OD_{600} of 0.08. *N. gonorrhoeae* liquid cultures were grown for 8 hours in a T75 flask in a shaking incubator set at 37°C and 170-200 RPM. Samples were removed each hour for the determination of optical density (OD_{600}), Western blot analysis, aconitase assays and real-time RT-/qPCR experiments as described below. Growth curves where strains never exited lag phase were not included and each experiment was repeated in at least triplicate unless otherwise noted. The arithmetic mean ± standard error is displayed unless otherwise noted.

E. coli samples DH5α cells were streaked from plates stored at 4°C onto LB agar plates and grown overnight at 37°C. Cells were swabbed and used to inoculate liquid LB media to give a starting OD_{600} of 0.08. *E. coli* liquid cultures were grown for 8 hours in a baffled 250mL Erlenmeyer flask. Samples were removed every other hour for determining optical density (OD_{600}) and after 8 hours (in stationary phase) samples were taken for aconitase activity assays

as described below.

3. Glucose Measurement

The glucose concentration of the media was measured at each time point using a Bayer Contour Next blood glucose monitor. A standard curve was generated using GCB liquid media with known concentrations of glucose to account for differences in conductivity between blood and GCB media.

4. RNA Extraction, RT-PCR and qPCR

The appropriate strains were grown in liquid GCB media with glucose as the carbon source. The equivalent of 10 mL of cells at OD_{600} 0.18 was removed at 2 and 3 hr (log phase) and at 7 and 8 hr (stationary phase) of growth, the bacteria were collected by centrifugation, re-suspended in RNAlater, and stored at 4°C. Total RNA from the cells was extracted the next day using the Bio-Rad Aurum Total RNA Mini Kit and eluted in 40µL RNase-free water. One µL of RNAsin (RNase inhibitor, Promega) was added to the extracted RNA and the total RNA concentration was determined using a Nanodrop reader. To remove any DNA contamination, 1 µg of total RNA was digested for approximately 40 minutes at 37°C with 1 unit of RQ1 RNase-free DNase (Promega). The DNase was inactivated using the supplied stop solution at 65°C for 10 minutes.

cDNA was generated from purified total RNA using the Bio-Rad iScript Reverse Transcription Supermix. Real-time qPCR was performed using the Bio-Rad Sso Advanced Universal SYBR Green Supermix, the oligonucleotides listed in Table 1, and the Bio-Rad CFX96 Touch Real-Time PCR Detection System. Fold change was determined using the $2^{-\Delta\Delta C_t}$ method [16] with 16S rRNA as the reference gene. RNA reference samples were diluted 1:50,000 using RNase-free water.

5. Western Blotting and Electrophoresis

Aliquots of *N. gonorrhoeae* liquid cultures were taken hourly starting at 2 hours of growth. The equivalent of 1 mL of cells at OD_{600} = 0.18 (i.e. 0.18 OD•mL) was pelleted, the supernatant was aspirated, and the samples were frozen at -20°C if not used immediately. Pellets were re-suspended in 100 µL fresh 1X Sample Buffer (0.07M Tris-HCl, pH 6.8, 10% Glycerol, 5% beta-mercaptoethanol, 1.05% SDS, dyed with Bromophenol Blue) and boiled for 5 minutes. Samples were centrifuged briefly and equal volumes of protein were loaded and resolved on a 10% polyacrylamide SDS-PAGE gel.

The proteins in the gel were transferred to a PVDF membrane and blocked in PBS-Tween (PBS with 0.1% Tween 100) containing 5% non-fat dry milk (NFDM) for 1 hour at room temperature on a shaker table. The membrane was incubated in PBS-Tween containing 2.5% NFDM and 1:10,000 rabbit PilM antibody for 1 hour at room temperature on a shaker table. The membrane was then washed four times for 9 minutes each in fresh PBS-Tween on a shaker table. The membrane was then incubated in PBS-Tween containing 2.5% NFDM, 1:1,000 3F10 (mouse HA antibody conjugated with HRP) and 1:20,000 goat anti-rabbit HRP-conjugated antibody for 1 hour at room temperature on a shaker table. The membrane was washed again as previously described and then incubated for 2 minutes with Bio-Rad ECL reagents and photographed using the Bio-Rad ChemiDoc Touch Imager. PilM was used as an internal loading control because its production does not appear to change in different phases of growth, however it was not used to normalize protein abundance between strains because its abundance appears to vary between strains.

6. Aconitase Activity Assays

Samples were prepared in a similar manner as described by Gardner [17] and Hausladen and Fridovich [18]. Strains were grown in liquid cultures with glucose as the carbon

source as previously described until they reached an OD_{600} 0.5 or until they had reached stationary phase (8 hours), at which point 10 OD•mL of cells were collected by centrifugation, re-suspended in 1 mL of Tris/BME Buffer (0.4M Tris-HCl pH 7.4, 5mM beta-mercaptoethanol) and pelleted again. Pellets were re-suspended again in 200µL of new Tri-BME, snap frozen in a dry ice bath and stored at -80°C for later use. Samples were thawed in RT water and snap frozen/thawed one more time for a total of two freeze/thaw cycles. Samples were then sonicated in an ice bath using a VirSonic 50 ultrasonic probe sonicator at 50% power for 6 15-sec pulses with 20-sec pauses between sonications. Samples were then snap frozen/thawed for an addition cycle and then spun in a TL-100 benchtop ultracentrifuge for 20 min at 40k rpm. The clear, soluble fraction of the lysate was removed to a clean tube and stored at -80°C for later use. FA19 samples were prepared from at least 2 biological replicates.

Aliquots of lysate were either treated with dipyridyl, reactivated, or left untreated. For dipriydyl treatment, 45µL of lysate was mixed with 6µL dipyridyl buffer (4.25mM dipyridyl, 5.525mM dextrose in water) and incubated on ice for 1 hr. Dipyridyl is a non-ionic iron chelator that inactivates aconitases [17]. For reactivation, 45µL of lysate was placed in a screw-capped tube, supplemented with 5µL 0.5M DTT, 0.5µL 20mM Na_2S and 0.5µL 20mM $(NH_4)_2Fe(SO_4)_2$, then placed under nitrogen, sealed with parafilm and incubated on ice for 30min. For untreated samples, 45µL of lysate was mixed with 6µL of dH_2O before being assayed.

The activity assays were performed quickly, particularly with reactivated samples, so that minimal aconitase activity was lost upon exposure to oxygen. First, 90µL of dH_2O was added to each well, then 10µL of lysate was added to the appropriate wells in a microtiter plate before 200µL of reaction mix was quickly added using a repeater pipette for a total volume of 300µL (Final Concentration: 50mM Tris-HCl (pH 7.4), 0.6mM $MnCl_2$, 0.2mM $NADP^+$, 20mM Sodium Citrate, 18µg/mL IDH). The linear increase in absorbance at 340nm during the first ~3.5 minutes of the reaction was measured and the molar extinction coefficient of NADPH (6.22 $x10^3$ $M^{-1}cm^{-1}$) was used to calculate the amount of aconitase activity present. One unit of aconitase activity

was defined as the generation of one μmole of NADPH per minute.

Protein concentration was determined using a modified Bio-Rad Bradford Protein Assay. Two, four, six, and eight μL of diluted samples and BSA standards were mixed with 40μL Bio-Rad Bradford Reagent and dH_2O to a final volume of 200μL in a microtiter plate. The plate was left to incubate at RT for 10 min and then the OD_{595} was measured. The ratio of the slopes between the BSA standard and the diluted protein samples was used to calculate the protein concentration of the samples.

For purified protein assays, the mutant and wild-type versions of the *N. gonorrhoeae* *acnB* gene were cloned into *E. coli*, overexpressed and purified. Immediately before measurement, the proteins were re-activated using Na_2S, Fe^{2+}, and DTT and kept under nitrogen prior to use. AcnB activity was measured by adding citrate or isocitrate and monitoring the formation of cis-aconitate at 240 nm. Aconitase activity assays on purified protein were performed by Josh Tomberg.

7. RNA Synthesis

The 5' UTR and extended 3 'UTR of the *acnB* mRNA from *N. gonorrhoeae* FA19 were cloned into the BamHI and XbaI sites next to the T7 promoter of pBSII KS+. The 5'UTR of *acnB* was defined as the region from -76 to +277. The extended 3'UTR was defined as from 28 bases upstream of the *acnB* stop codon to 295 bases downstream of the *acnB* stop codon. Plasmids were transformed into *E. coli* MC1061 cells and were purified using the Invitrogen Plasmid Miniprep Kit. Purified plasmids were linearized with BamHI and the RNA was transcribed using the NEB HiScribe T7 In Vitro Transcription Kit. Transcripts were purified using the Qiagen RNeasy Mini Kit and 1 μL of RNAsin (RNase inhibitor, Promega) was added per 40μL of recovered RNA. RNA quality was qualitatively confirmed by running the transcripts and supplied positive control on a 1% agarose TAE gel. The RNA concentration was found using a Nanodrop reader. The cloned *tssA1* RNA from *Pseudomonas aeruginosa* from Marden et al. [19] was

used as the RNA in the positive control with RsmA protein for the EMSAs.

8. Electrophoretic Motility Shift Assays (EMSAs)

AcnB purified protein was inactivated by incubating the enzyme with a 50-fold molar excess of EDTA and 20-fold molar excess of Potassium Ferricyanide for 6 minutes on ice. The inactivated AcnB protein (Apo-AcnB) was purified again using size-exclusion chromatography. The RsmA protein from *P. aeruginosa* from Marden et al. [19] was used as the positive control protein with *tssa1* RNA transcribed *in vitro*.

An EMSA was set up so that 70ng of RNA was incubated with various amounts of protein (see Figures 12 and 13) in 10mM Tris-Cl (pH 7.5), 10mM $MgCl_2$, 100mM KCl, 5% glycerol, 10mM DTT, and 0.25µL RNasin to a final volume of 10µL and incubated at 37°C for 30 min. The mixture was then supplemented with 2µL 6X Invitrogen (EMSA) gel-loading solution and immediately loaded onto a non-denaturing 5% polyacrylamide gel and resolved. The running buffer (10mM Tris-Cl, 300mM Glycine, 1mM EDTA) was prepared ahead of time and stored at 4°C. The gel was also pre-run at 200V for 30 minutes and the gel apparatus was kept in an ice bath to keep it cold.

The finished gel was then incubated with 1X SYBR Green (Nucleic Acid Dye) in 1X TBE buffer in the dark for 30 minutes, washed three times for 10 seconds with dH_2O and imaged using the Bio-Rad ChemiDoc Touch Imager. The same gel was then incubated in SYPRO Ruby (Protein) Stain for 3 hours in the dark, washed three times for 10 seconds with dH_2O, destained with 10% methanol/7% acetic acid for one hour, washed three times for 10 seconds with dH_2O again and then imaged using the Bio-Rad ChemiDoc Touch Imager.

Results

1. Growth Phenotypes

Five strains were examined for their growth phenotypes: FA19 *rpsL*, FA19 *rpsL penA41*, FA19 *rpsL acnB*-G348D, FA19 *rpsL penA41 acnB*-G348D, and the compensatory mutant strain LV41C (Figure 1). The *rpsL* gene confers streptomycin resistance and is necessary for colonization in the mouse model of gonococcal infection [20]. Importantly, the two strains containing the *acnB*-G348D mutation, FA19 *rpsL penA41 acnB*-G348D and FA19 *rpsL acnB*-G348D, mirrored the growth phenotype of LV41C. These strains demonstrated an increased growth rate during log phase as compared to FA19 *rpsL penA41* and a lower OD_{600} in stationary phase as compared to FA19 *rpsL* and FA19 *rpsL penA41*. After entering stationary phase, both *acnB*-G348D strains experienced a slight decrease in OD_{600} (Figure 1). Strains containing the *acnB*-G348D mutation also had an increased growth rate during log phase and decreased OD_{600} in stationary phase relative to FA19 *rpsL* and FA19 *rpsL penA41* when grown in media containing lactate instead of glucose; however, the overall growth rate of all strains was reduced (Figure 2). These data indicate that introduction of the *acnB*-G348D mutation is both necessary and sufficient to phenocopy the growth characteristics of the original spontaneous compensatory mutant LV41C.

2. Glucose Consumption

Since detectable levels of aconitase activity in *N. gonorrhoeae* have been reported to be present only when glucose has been depleted [12], the glucose consumption during liquid growth was determined for three strains, FA19 *rpsL*, FA19 *rpsL penA41 acnB*::kan, and LV41C (Figure 3). Glucose levels remained relatively stable for about 3 hours, then showed a linear decline to 10-15 mM at the end of 8 hrs, and there were no noticeable changes in glucose consumption when transitioning from log phase to stationary phase. Neither FA19 *rpsL penA41 acnB::kan* nor LV41C showed any difference in the pattern of glucose consumption compared to

FA19 *rpsL*. There was no complete glucose depletion observed, even after 8 hours of growth (Figure 3).

3. Relative AcnB Protein Abundance

The report that AcnB activity was only present in glucose-depleted conditions in *N. gonorrhoeae* suggested a complex, phase-dependent regulation of AcnB; therefore, I assessed AcnB protein production throughout the growth cycle. Equal amounts of OD•mL from strains producing HA-tagged AcnB, FA19 *rpsL acnB*-HA, FA19 *rpsL acnB*-G348D-HA, FA19 *rpsL penA41 acnB*-HA and FA19 *rpsL penA41 acnB*-HA, were sampled hourly starting at the beginning of logarithmic growth (t=2 hr) and ending at stationary phase growth (t=8 hr) and prepared for SDS-PAGE Following electrophoresis, the separated proteins were transferred to PVDF membranes and blotted with 3F10 antibody to identify HA-tagged proteins. Strains producing the AcnB-G348D mutant had a 5- to 10-fold decrease in AcnB protein production compared to those containing an HA-tagged wild-type AcnB at t=2 hr. The addition of the *penA41* allele alone did not significantly alter the amount of AcnB protein compared to the strain with wild-type *acnB* gene (Figure 4). When the levels of WT and mutant AcnB were normalized to the levels at t=2 hr of growth, strains FA19 *rpsL acnB*-HA and FA19 *rpsL acnB*-G348D-HA showed consistent AcnB abundance throughout log phase growth, but as the strains transitioned into stationary phase, the wild-type AcnB protein abundance increased 2- to 3-fold, whereas the mutant AcnB abundance decreased 2- to 3-fold (Figure 5).

The addition of the *penA41* allele in strains with the wild-type *acnB* gene did not appear to prevent the increase of AcnB protein from log to stationary phase. The effect of the *penA41* allele in strains with a mutant *acnB* gene was indeterminate (Figure 6).

4. Relative *acnB* mRNA Expression

In other species, AcnB is known to bind to its own transcript to regulate the translation

and degradation of its own message [21]. To determine if the variations in protein abundance during *in vitro* growth (Figure 5) could be explained by differences in mRNA levels, RT/qPCR was performed on total RNA isolated cells from cells harvested from log phase (t=2, 3) and stationary phase (t=7, 8) growth. There was no change in *acnB* mRNA expression observed between log phase growth and stationary phase growth in strains expressing either the wild-type or mutant *acnB* gene (Figure 7, 8). Compared to the wild-type *acnB* strain, the mutant strain had just over a 2-fold increase in *acnB* mRNA in both stationary and log phases of growth (Figure 9).

5. Aconitase Activity

To ascertain the effect of the G348D mutation on the aconitase activity of the enzyme itself, we measured the formation of cis-aconitate from either citrate or isocitrate by quantifying the increase in absorbance at 240 nm. The initial rates of aconitate formation were plotted at different citrate or isocitrate concentrations, and the Vmax and Km constants were derived (Figure 10, experiment performed by Josh Tomberg). The mutant AcnB protein showed a 2.6-fold reduction of the Vmax in the direction of citrate → cis-aconitate and a 3.2-fold reduction of the Vmax in the direction isocitrate → cis-aconitate compared to the wild-type protein.

I also determined the amount of aconitase activity present in cell lysates of liquid cultures of FA19 *rpsL* harvested at log phase and stationary phase growth. I measured the amount of citrate converted to isocitrate indirectly by quantifying the increase in absorbance at 340nm due reduction of $NADP^+$ to NADPH by isocitrate dehydrogenase in samples supplemented with citrate and excess isocitrate dehydrogenase. There was approximately 7.5 mU of aconitase activity/mg of soluble protein (95% CI 5.7-9.3 mU/mg) in log phase-reactivated FA19 *rpsL* lysates and 7.0 mU/mg of activity (95% CI 6.4-7.6 mU/mg) in stationary phase-reactivated FA19 *rpsL* lysates. There was minimal or no aconitase activity detected in FA19 lysates that were not reactived or were dipyridyl-treated. For reference, reactivated stationary

phase *E. coli* lysates had 39.7 mU/mg of activity (95% CI 36.6-42.9 mU/mg) and in unactivated and dipyridyl-treated lysates there was approximately 2.7 and 1.9 mU/mg of activity, respectively (Figure 11). There was no difference in aconitase activity detected in reactivated samples (i.e. treated with Na_2S, Fe^{2+}, and dithiothreitol) from log and stationary phase samples of FA19 *rpsL* liquid cultures and all aconitase activity was lost in processed samples that were not reacitvated. Overall, *E. coli* liquid cultures exhibited more than 5-fold more aconitase activity per mg of soluble protein than FA19 *rpsL* liquid cultures.

6. EMSA

In other species, aconitase can function as a posttranscriptional regulator by binding to the 5' or 3' UTRs of mRNAs, including its own mRNA [21] [22]. To ascertain if there was any binding between *acnB* mRNA and AcnB protein that could explain the relationship between protein abundance and mRNA expression, electrophoretic motility shift assays were performed using the 5' and 3' UTRs of *acnB* mRNA and apo-AcnB protein. Apo-AcnB was used because the apo-enzyme state is necessary for mRNA binding in other aconitases [21]. We detected no observable shift or overlap in RNA and/or protein (Figures 12 and 13), although there was overlap in the positive control protein, RsmA, and its binding mRNA, *tssa1*, along with a shift in both the RsmA protein and *tssa1* mRNA bands. These data suggest there was no binding detected between either the 5' UTR or 3' UTR of *acnB* mRNA and Apo-AcnB protein. Future experiments will be necessary to determine unequivocally if apo-AcnB can bind to *acnB* mRNA.

Discussion

1. Growth Phenotype

The stationary phase of bacterial growth is often caused by depletion of resources below a threshold or by signaling molecules from other bacteria that indicate a bacterial population has reached critical density. Usually, exhaustion below a relative threshold of only one essential nutrient is sufficient for stationary phase to occur [23]. Pyruvate, lactate, and glucose are the only 3 carbon sources that can be efficiently utilized by *N. gonorrhoeae*, with the latter two being the only ones that are common and readily available in vaginal fluid [24] [10]. Previous studies have shown that *N. gonorrhoeae* undergoes a metabolic shift after the depletion of glucose, which might be classically associated with stationary phase [12]. In these experiments, there was no complete depletion of glucose as the bacteria entered stationary phase for any strain, suggesting that the stationary phase was not caused by a total depletion of glucose. However, our data do not rule out that entrance into stationary phase was initiated when glucose levels, while not absent, dropped below a certain threshold. Similarly, since lactate did not alter the growth phenotype in *acnB* mutants, the availability of different carbon sources did not appear to influence the growth phenotypes.

2. Function of AcnB as a TCA enzyme in *N. gonorrhoeae*

E. coli has at least two functional aconitases, AcnA and AcnB [21]. AcnB is the primary aconitase enzyme during logarithmic growth, whereas the more oxidatively stable AcnA is produced during stationary growth. In *N. gonorrhoeae,* the *acnA* gene contains a frameshift mutation that generates a premature stop codon. This protein is not produced at any observable levels and, even after the gene is repaired and placed under a promoter that should allow AcnA to be constitutively produced, production of the AcnA protein is not observed (data not shown; experiments performed by Josh Tomberg). Thus, AcnB is the only known functional aconitase in

N. gonorrhoeae.

Interestingly, the early entrance into stationary phase growth and even the slight decline in OD_{600} is a direct consequence of the marked decrease of aconitase activity. In *N. gonorrhoeae*, aconitase activity has been reported to become active once acetate in the medium is imported, converted to acetyl-CoA, and then condensed with oxaloacetate to generate citrate. Because strains containing the *acnB*-G348D mutation have i) a 5- to 10-fold reduction in abundance in log phase, ii) a 30- to 80-fold reduction in abundance in stationary phase, and iii) a 3-fold reduction in activity relative to strains producing wild-type AcnB, it would appear that the *acnB*-G348D mutation acts as a functional knockout with regards to the activity of AcnB in the TCA cycle. The absence of production of AcnB-G348D in stationary phase and the lower activity of AcnB-G348D in enzymatic assays suggest that the stationary phase levels of aconitase activity in the mutant are severely decreased, which is consistent with the growth phenotype of strains harboring the mutant *acnB* allele. It is reasonable to conclude that upon entering stationary phase, the wild-type AcnB protein is up-regulated in order to maximize energy generation and therefore increases the number of cells that can be sustained in stationary phase, thus leading to a difference in OD_{600} in stationary phase compared to mutant strains. Although the activity assays did not show a significant difference in aconitase activity between log phase and stationary phase, it is possible that the assay is not sensitive enough to detect the difference between log and stationary phase activity, or more likely that normally inactive protein is reactivated by the assay procedure. The lack of detail in the methods section of Hebler and Morse [12] and the extremely sensitivity of AcnB to oxidation [17] made it difficult to address this question in the time available, but this remains an interesting phenomenon worthy of further study.

The compensatory mutant LV41C does show a sharp decrease in CFU after entering stationary phase whereas the parent strain plateaus, indicating that decrease in OD_{600} during stationary phase associated with the growth phenotype is possibly due to cell lysis instead of

altered optical characteristics or clumping. Clumping is excluded because the *opa* genes (adhesins that cause clumping) did no show significantly altered expression in the mutants and only non-piliated colonies were used (data not shown; experiments performed by Leah Vincent and Yang Tan).

3. Post-transcriptional regulation

There was a clear discrepancy between the levels of AcnB protein and the levels of *acnB* mRNA. The levels of *acnB* mRNA remained constant in the strains tested from log- and stationary-phase cultures, whereas the levels of AcnB protein changed quite dramatically in both wild-type and mutant strains as the cells transitioned from log-phase to stationary-phase growth. Compared to the wild-type, the mutant strain paradoxically had more overall *acnB* mRNA, but a reduction in the amount of protein produced.

In *E. coli* and *Helicobacter pylori*, AcnB has been reported to act as a post-transcriptional regulator of protein production by binding to the UTRs of multiple mRNAs, including its own, and altering the translation rates of translation of the bound RNA [21] [22]. These reports hint at a possible post-transcriptional mechanism in *N. gonorrhoeae* that may regulate AcnB protein production. Given that aconitase functions as a pleiotropic post-transcriptional regulator in other species, it is possible that the aconitase in *N. gonorrhoeae* is functioning as a post-transcriptional regulator as well. Although the EMSAs did not indicate binding between the Apo-AcnB protein and the 3'UTR or 5'UTR of *acnB* mRNA, it is possible that the optimal reaction conditions for this interaction were not used or that AcnB could be altering the production of itself indirectly through the regulation of other transcripts. With regards to the former possibility, binding conditions similar to those used by Tang and Guest [21] and Austin et al. [22] were also used and did not have any observable shifts in motility for the combinations of RNA and AcnB tested (data not shown). It is also possible that the binding of AcnB protein to other transcripts is more important for fitness in the compensatory mutant because approximately 65 genes are

upregulated more than 2-fold in *acnB* mutant strains during logarithmic growth on glucose (data not shown; experiments performed by Yang Tan).

In conclusion, the mechanism by which the *acnB*-G348D mutant allele compensates for some of the biological fitness cost associated with carrying the mosaic *penA41* allele is unclear, but it does not appear to be directly related to its function as a TCA cycle enzyme. One possibility is that the mutant protein functions as a post-transcriptional regulator, thereby regulating production of other proteins and expression of other genes. Indeed, of the 65 genes upregulated in strains harboring the *acnB*-G348D mutant allele at log-phase growth, 2/3 of them are in energy production and carbon metabolism, and this upregulation may be sufficient to confer a fitness advantage. Moreover, given the constant levels of glucose and lactate present in the vaginal tract, infections in the host are unlikely to encounter physiological conditions that would trigger entrance into stationary-phase growth where the fitness of the mutant strains might be compromised.

Literature Cited

[1] M Cohen et al., "Reduction of concentration of HIV-1 in semen after treatment of urethritis: implications for prevention of sexual transmission of HIV-1," *Lancet*, vol. 348, pp. 1868-1873, 1997.

[2] D Fleming and J Wasserheit, "From epidemiological synergy to public health policy and practice: the contribution of other sexually transmitted diseases to sexual transmission of HIV infection," *Sex Trans Infect*, vol. 74, no. 1, pp. 3-17, 1999.

[3] Centers for Disease Control and Prevention, ""Sexually Transmitted diseases treatment guidelines, 2015"," *MMWR Morb Mortal Wkly Rep 2015*, vol. 64, no. RR-3, pp. 1-137, 2015.

[4] D Golparian et al., "High-level cefixime- and ceftriaxone resistant N. gonorrhoeae in France: Novel penA mosaic Allel in successful international clone causes treatment failure," *Antimicrob Agents Chemother*, vol. 56, pp. 1273-1280, 2011.

[5] J Tomberg, M Unemo, M Ohnishi, C Davies, and R Nicholas, "Identification of amino acids conferring high-level resistance to expanded-spectrum cephalosporins in the penA gene from Neisseria gonorrhoeae strain H041.," *Antimicrob Agents Chemother*, vol. 57, no. 7, pp. 3029-3036, July 2013.

[6] N Händel, J Schuurmans, S Brul, and B ter Kuile, "Compensation of the Metabolic Costs of Antibiotic Resistance by Physiological Adaptation in Escherichia coli," *Antimicrob Agents Chemother*, vol. 57, no. 8, pp. 3752-3762, Aug 2013.

[7] D Anderson, "The biological cost of mutational antibiotic resistance: any practical conclusions?," *Current Opinion in Microbiology*, vol. 9, no. 5, pp. 41-46, October 2006.

[8] J Björkman, I Nagaev, O Berg, D Hughes, and D Andersson, "Effects of Environment on Compensatory Mutations to Ameliorate Costs of Antibiotic Resistance," *Science*, vol. 287, no. 5457, pp. 1479-1482, 2000.

[9] S Gagneux et al., "The Competitive Cost of Antibiotic Resistance in Mycobacterium tuberculosis," *Science*, vol. 312, no. 5782, pp. 1944-1946, 2006.

[10] D Owen and D Katz, "A vaginal fluid simulant," *Contraception*, vol. 59, no. 2, pp. 91-95, February 1999.

[11] S Morse, S Stein, and J Hines, "Glucose Metabolism in Neisseria gonorrhoeae," *J. Bacteriol.*, vol. 120, no. 2, pp. 702-714, 1974.

[12] B Hebeler and S Morse, "Physiology and Metabolism of Pathogenic Neisseria: Tricarboxylic Acid Cycle Activity in Neisseria gonorrhoeae," *J Bacteriol*, vol. 128, no. 1, pp. 192-201, October 1976.

[13] A Wolfe, "The Acetate Switch," *Microbiology And Molecular Biology Reviews*, vol. 69, no. 1, pp. 12-50, 2005.

[14] R Fischer, G Martin, P Rao, and R Jensen, "Neisseria gonorrhoeae possesses two nicotinamide adenine dinucleotide-independent lactate dehydrogenases," *FEMS Microbiology Letters*, vol. 115, pp. 39-44, 1994.

[15] D Kellogg, W Peacock, W Deacon, L Brown, and C Pirkle, "Neisseria Gonorrhoeae I. Virulence genetically linked to clonal variation," *Journal of Bacteriology*, vol. 85, no. 6, pp.

1274-1279, 1963.

[16] A Lewis and K Rice, "Quantitative Real-Time PCR (qPCR) Workflow for Analyzing Staphylococcus aureus Gene Expression," in *The Genetic Manipulation of Staphylococci: Methods and Protocols*, J Bose, Ed. New York: Methods Mol Biol, 2016, pp. 143-154.

[17] P Gardner, "Aconitase: Sensitive target and measure of superoxide," *Methods in Enzymology*, vol. 349, pp. 9-23, 2002.

[18] A Hausladen and I Fridovich, "Measuring Nitric Oxide and Superoxide: Rate Constants for Aconitase Reactivity," *Methods in Enzymology*, vol. 269, pp. 37-41, 1996.

[19] J Marden et al., "An Unusual CsrA Family Member Operates in Series with RsmA to Amplify Posttranscriptional Responses in Pseudomonas Aeruginosa.," *Proceedings of the National Academy of Sciences of the United States of America*, vol. 110, no. 37, pp. 15055-15060, 2013.

[20] A Jerse, "Experimental Gonococcal Genital Tract Infection and Opacity Protein Expression in Estradiol-Treated Mice," *Infect Immun*, vol. 67, no. 11, pp. 5699–5708, 1999.

[21] Y Tang and J Guest, "Direct evidence for mRNA binding and post-transcriptional regulation by Escherichia coli aconitases," *Microbiology*, vol. 145, pp. 3069-3079, 1999.

[22] C Austin, G Wang, and R Maier, "Aconitase Functions as a Pleiotropic Posttranscriptional Regulator in Helicobacter pylori," *J. Bacteriol.*, vol. 197, no. 19, pp. 3076-3086, 2015.

[23] R Kolter, D Siegele, and A. Tormo, "The Stationary Phase of the Bacterial Life Cycle," *Annu Rev Microbiol*, vol. 145, no. 4, pp. 855-874, 1993.

[24] S Morse and L Bartenstein, "Factors affecting autolysis of Neisseria gonorrhoeae," *Proc Soc Exp Biol Med*, vol. 145, no. 4, pp. 1418-1421, April 1974.

[25] A Perkins and W Nicholson, "Uncovering New Metabolic Capabilities of Bacillus subtilis Using Phenotype Profiling of Rifampin-Resistant rpoB Mutants," *J. Bacteriol.*, vol. 190, no. 3, pp. 807-814, February 2008.

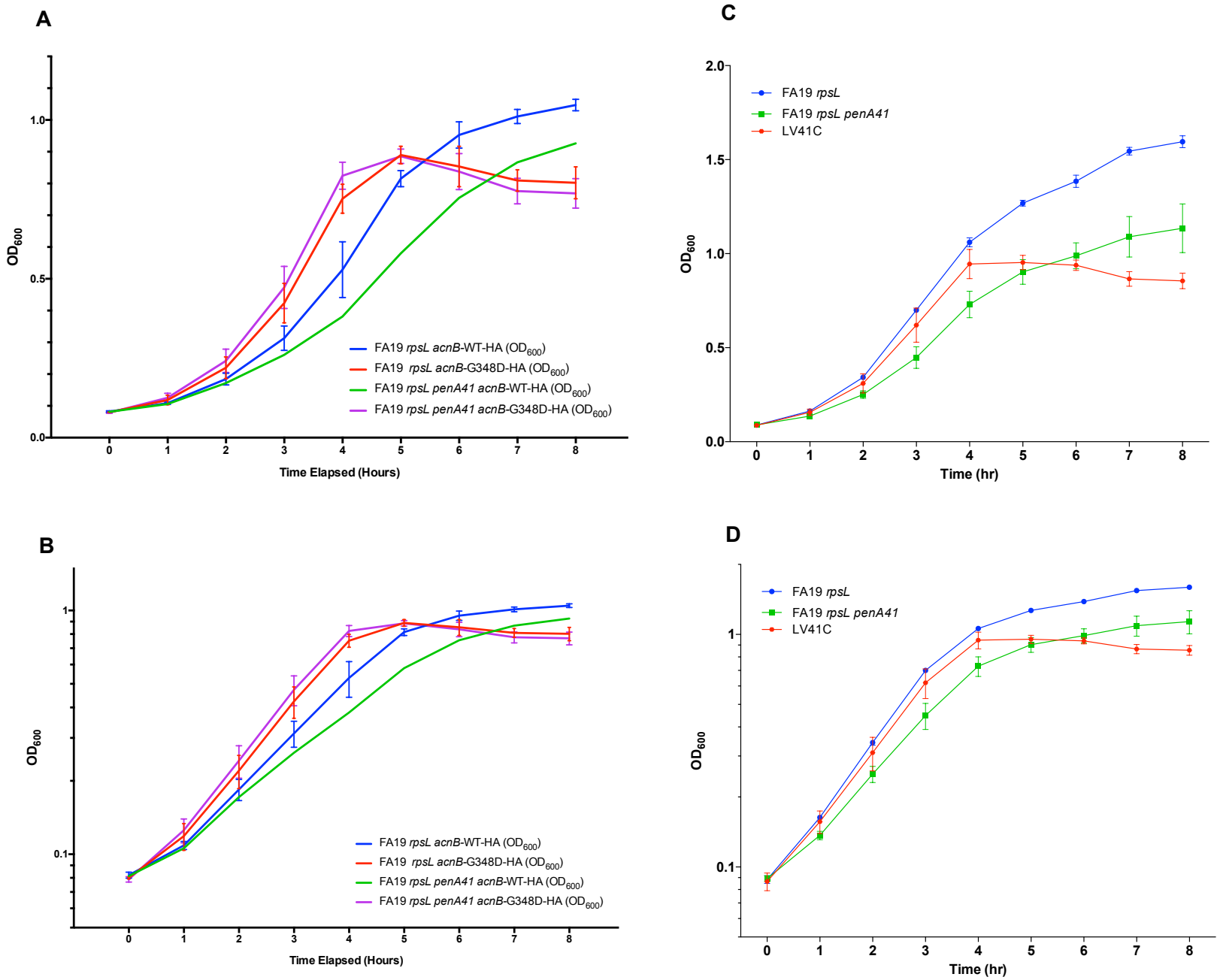

Figure 1

In vitro growth curves of the indicated *N. gonorrhoeae* strains in GCB liquid media with glucose as the carbon source. In A and B only one replicate of FA19 *rpsL penA41 acnB*-HA is presented, but is representative of the growth phenotype. Strains labeled with "-HA" are producing a HA-tagged AcnB. (A, C) Data on a linear scale (B, D) Data on a $\log_{10}$ scale. Experiments represented in C, D were performed by Leah Vincent at Uniformed Services University.

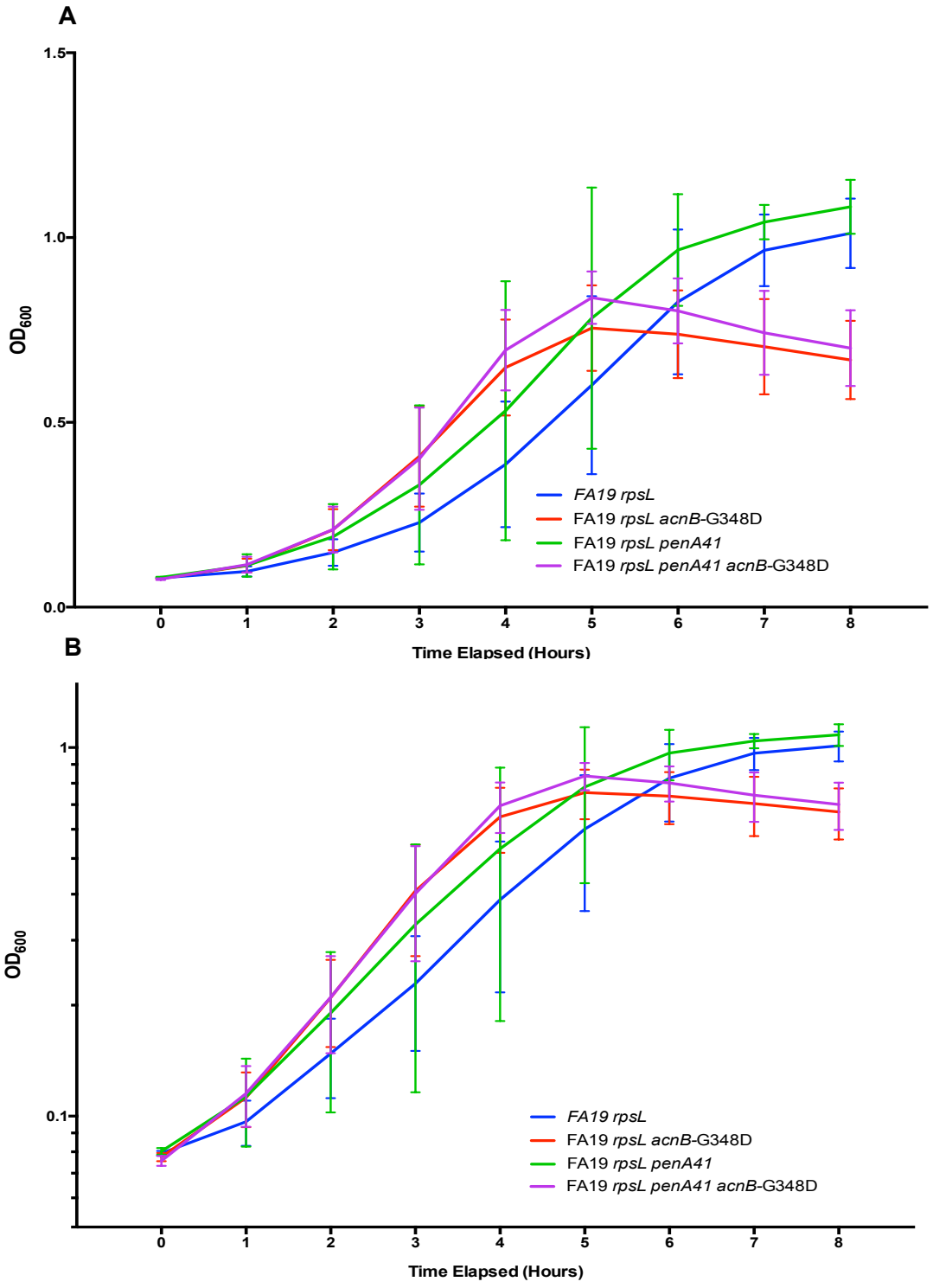

Figure 2

In vitro growth curves of the indicated *N. gonorrhoeae* strains in GCB liquid media with lactate as the carbon source. (A) OD_{600} plotted on a linear scale (B) OD_{600} plotted on a log_{10} scale

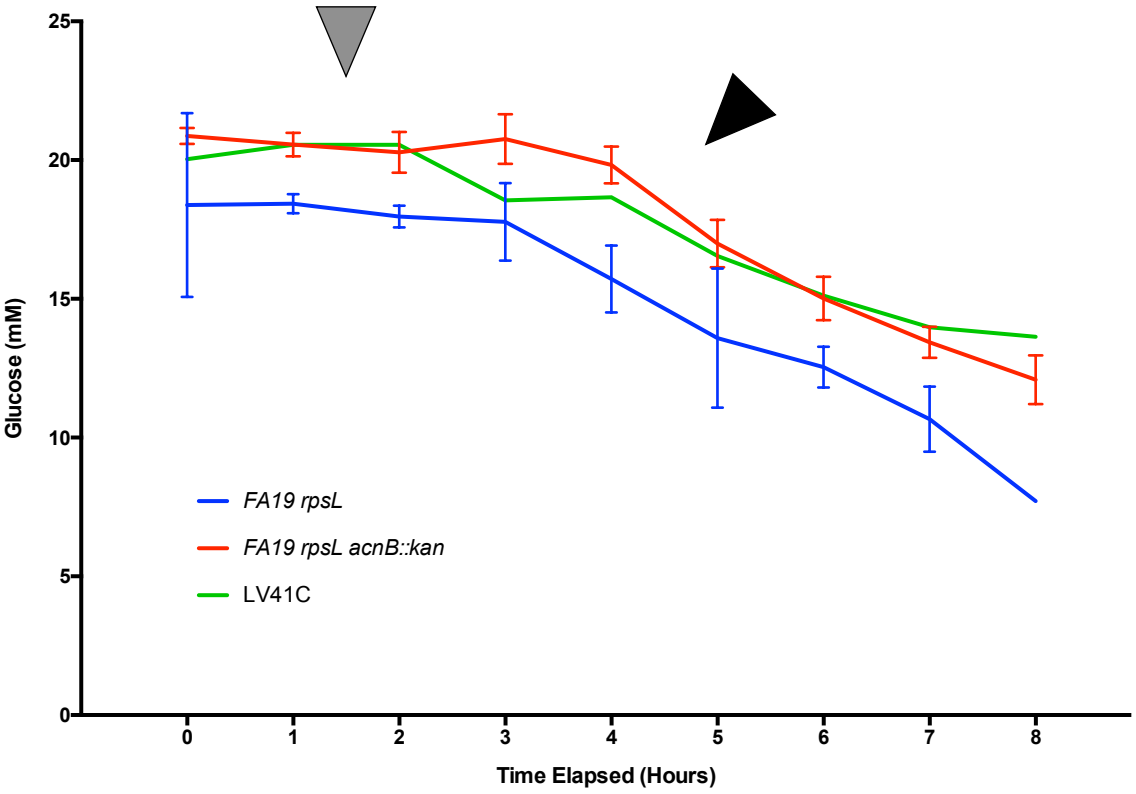

Figure 3
Glucose concentration in the media during *in vitro* growth of indicated *N. gonorrhoeae* strains in GCB liquid media with glucose as the carbon source. The grey marker indicates the approximate transition from lag to log phase and the black marker indicates the approximate transition from log to stationary phase. Only one replicate of LV41C is displayed. Four replicates of FA19 *rpsL* and three replicates FA19 *rpsL acnB*::*kan* are displayed.

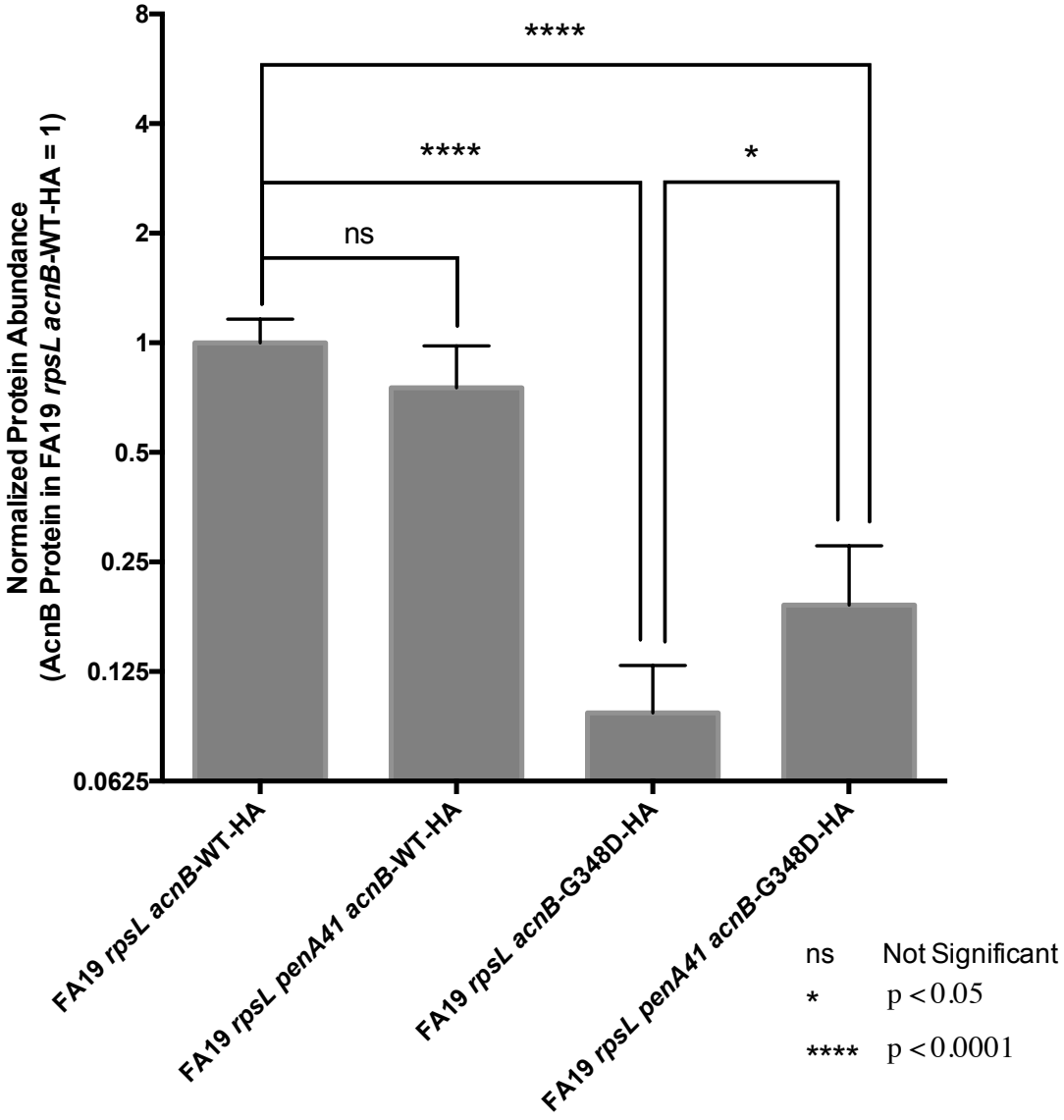

Figure 4
Relative abundance of AcnB in the indicated *N. gonorrhoeae* strains at the beginning of logarithmic growth *in vitro* (t=2 hr) using liquid GCB media with glucose as the carbon source. Data on a $\log_2$ scale.

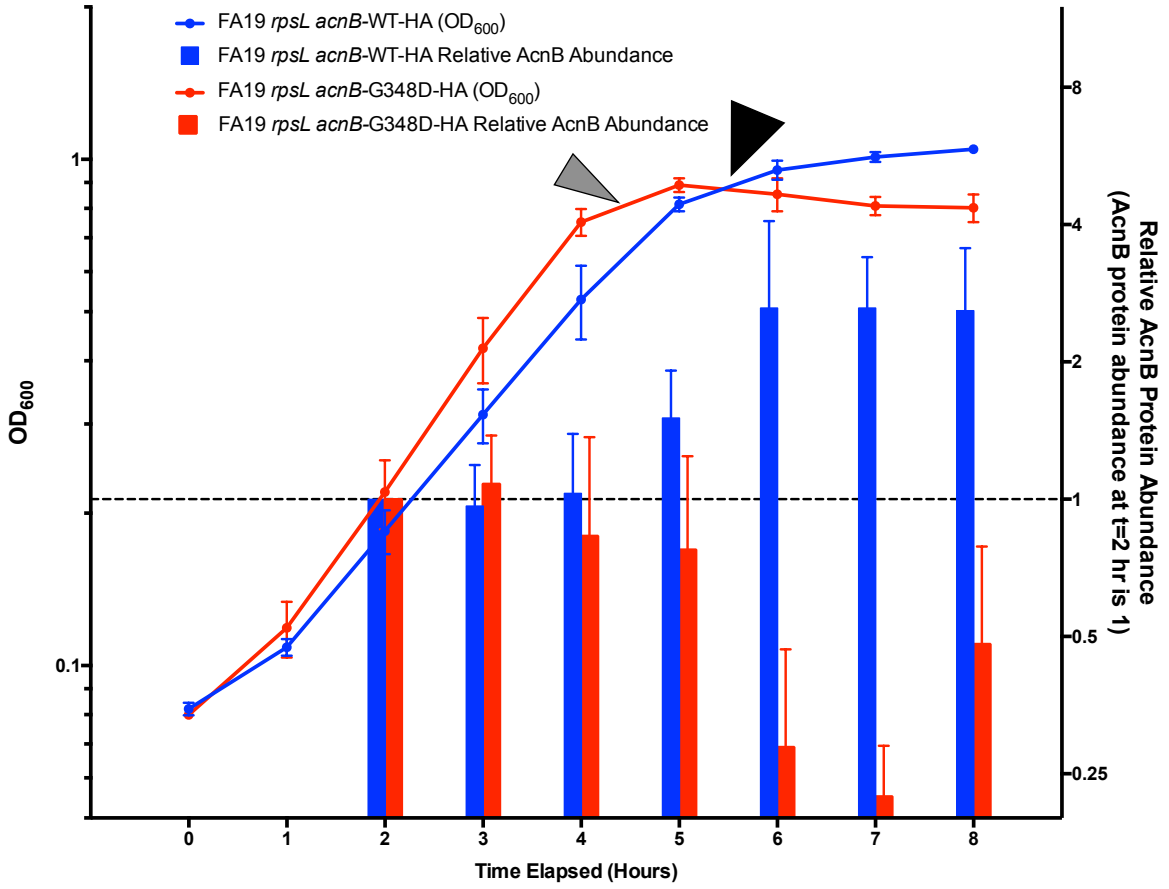

Figure 5

Growth curves and relative abundance of AcnB protein in two strains of *N. gonorrhoeae* during *in vitro* growth in liquid GCB media. Abundance is relative to the amount of protein present at the beginning of logarithmic growth (t=2 hr). Black marker indicates the transition from log to stationary phase for FA19 *rpsL acnB*-HA. Grey marker indicates the transition from log to stationary phase for FA19 *rpsL acnB*-G348D-HA. The left y-axis is on a $\log_{10}$ scale and the right y-axis is on a $\log_2$ scale.

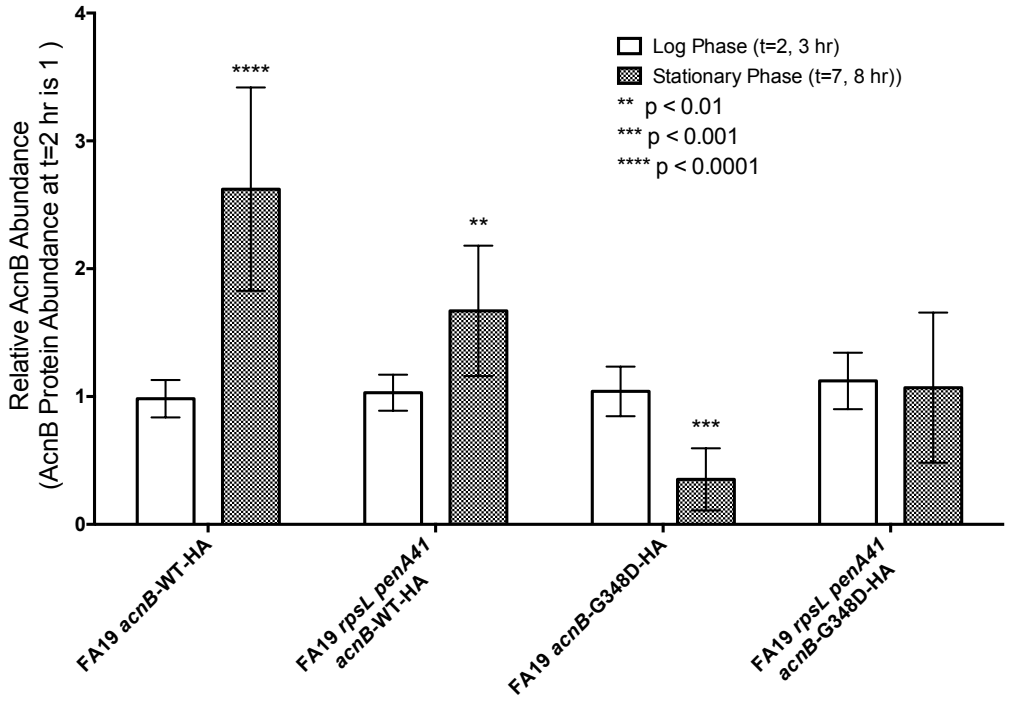

Figure 6

Comparative abundance of AcnB protein in stationary and log phases of growth in indicated *N. gonorrhoeae* strains during *in vitro* growth in liquid GCB media containing glucose as the carbon source. Abundance is relative to the amount of AcnB protein at the beginning of logarithmic growth (t=2 hr).

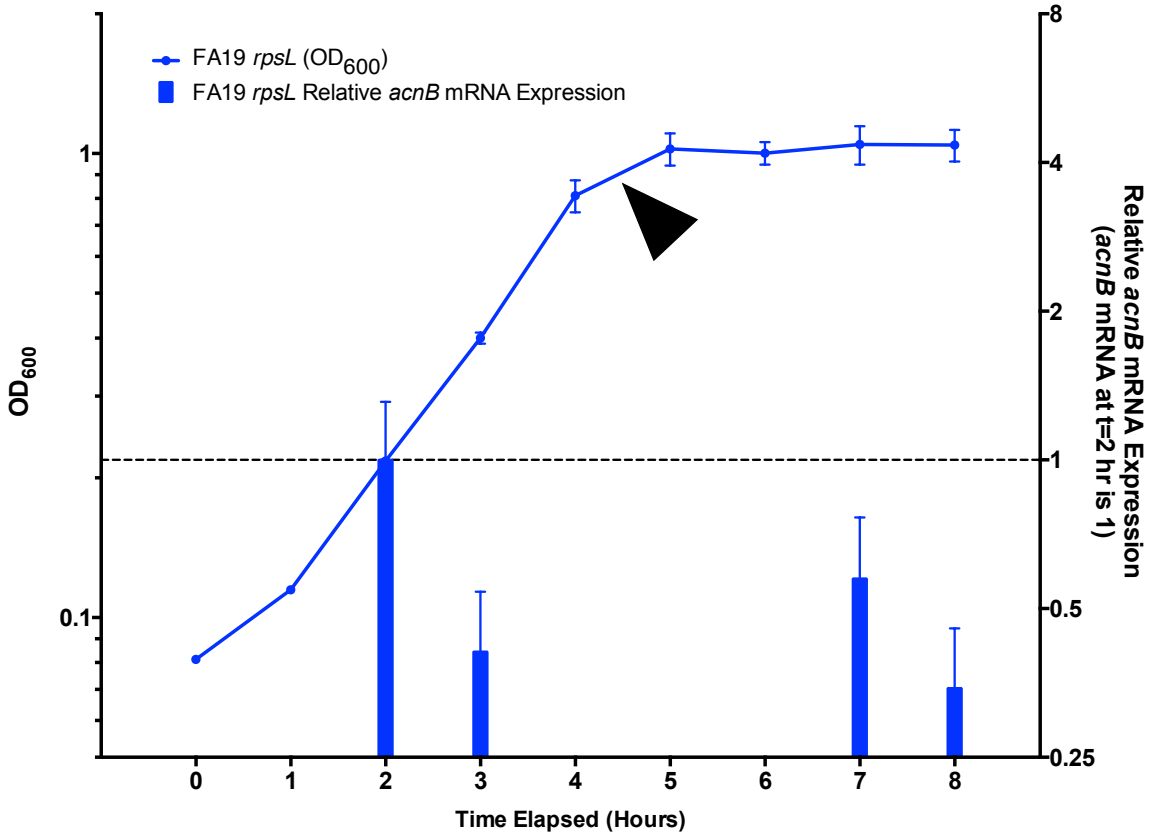

Figure 7

Expression of *acnB* mRNA in strains carrying the *acnB* wild-type allele. Expression is relative to the amount of mRNA at the beginning of logarithmic growth (t=2 hr). The black marker indicates the transition from log to stationary phase. Error bars for RNA expression represent the 95% CI. The left y-axis is on a $\log_{10}$ scale and the right y-axis is on a $\log_2$ scale.

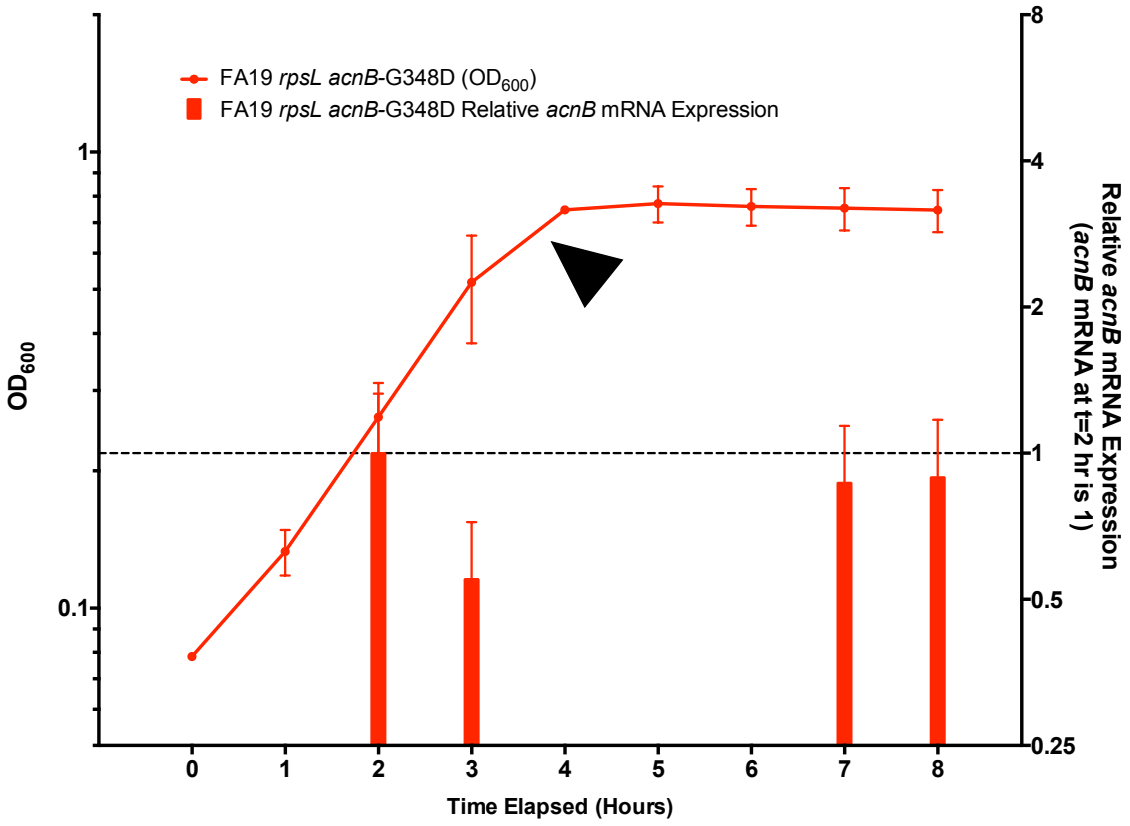

Figure 8

Expression of *acnB* mRNA in strains carrying the *acnB*-G348D allele. Expression is relative to the amount of mRNA at the beginning of logarithmic growth (t=2 hr). The black marker indicates the transition from log to stationary phase. Error bars for RNA expression represent the 95% CI. The left y-axis is on a $\log_{10}$ scale and the right y-axis is on a $\log_2$ scale.

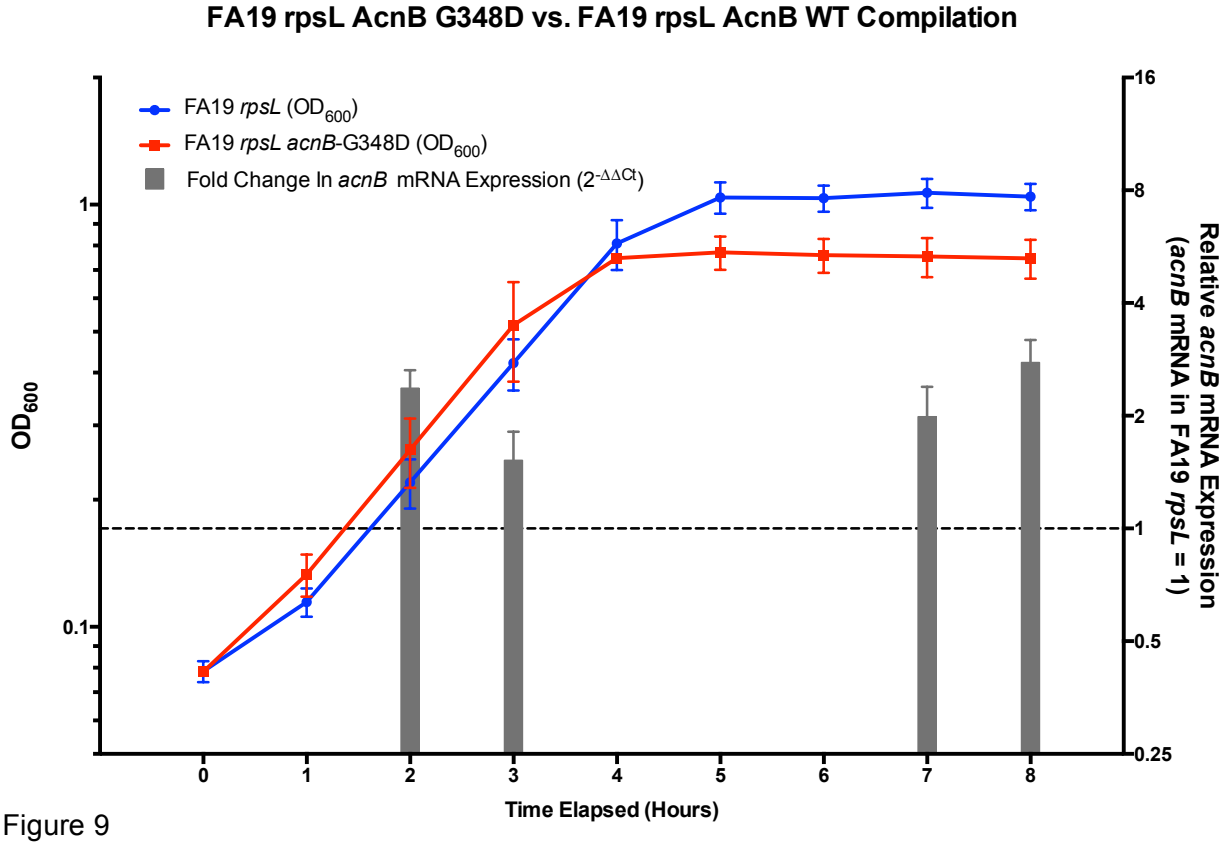

Figure 9

Expression of *acnB* mRNA in FA19 *rpsL acnB*-G348D relative to *acnB* mRNA in strains with the wild-type *acnB* allele during *in vitro* growth in liquid GCB media containing glucose as the carbon source. Error bars for RNA expression represent the 95% CI. The left y-axis is on a $\log_{10}$ scale and the right y-axis is on a $\log_2$ scale.

Citrate➔*cis*-Aconitate

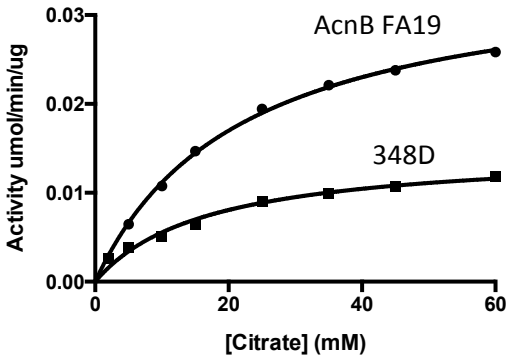

AcnB FA19 V_{max} = .0371 (n=5)
AcnB 348D V_{max} = .0145 (n=4)

2.6 fold reduction

AcnB FA19 K_m = 21.9
AcnB 348D K_m = 16.5

Isocitrate➔*cis*-Aconitate

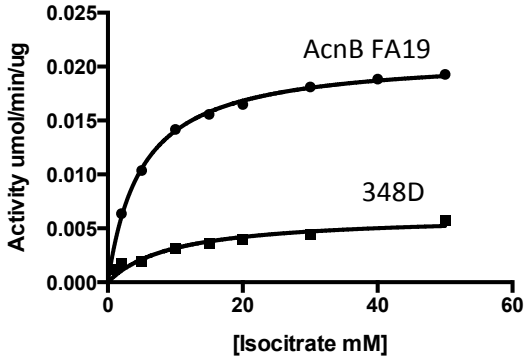

AcnB FA19 V_{max} = .0214 (n=4)
AcnB 348D V_{max} = .00667 (n=5)

3.2 fold reduction

AcnB FA19 K_m = 5.0
AcnB 348D K_m = 10.3

Josh Tomberg, UNC

Figure 10
Aconitase activity assay of mutant and WT AcnB proteins using purified, cloned proteins. Data generated by Josh Tomberg.

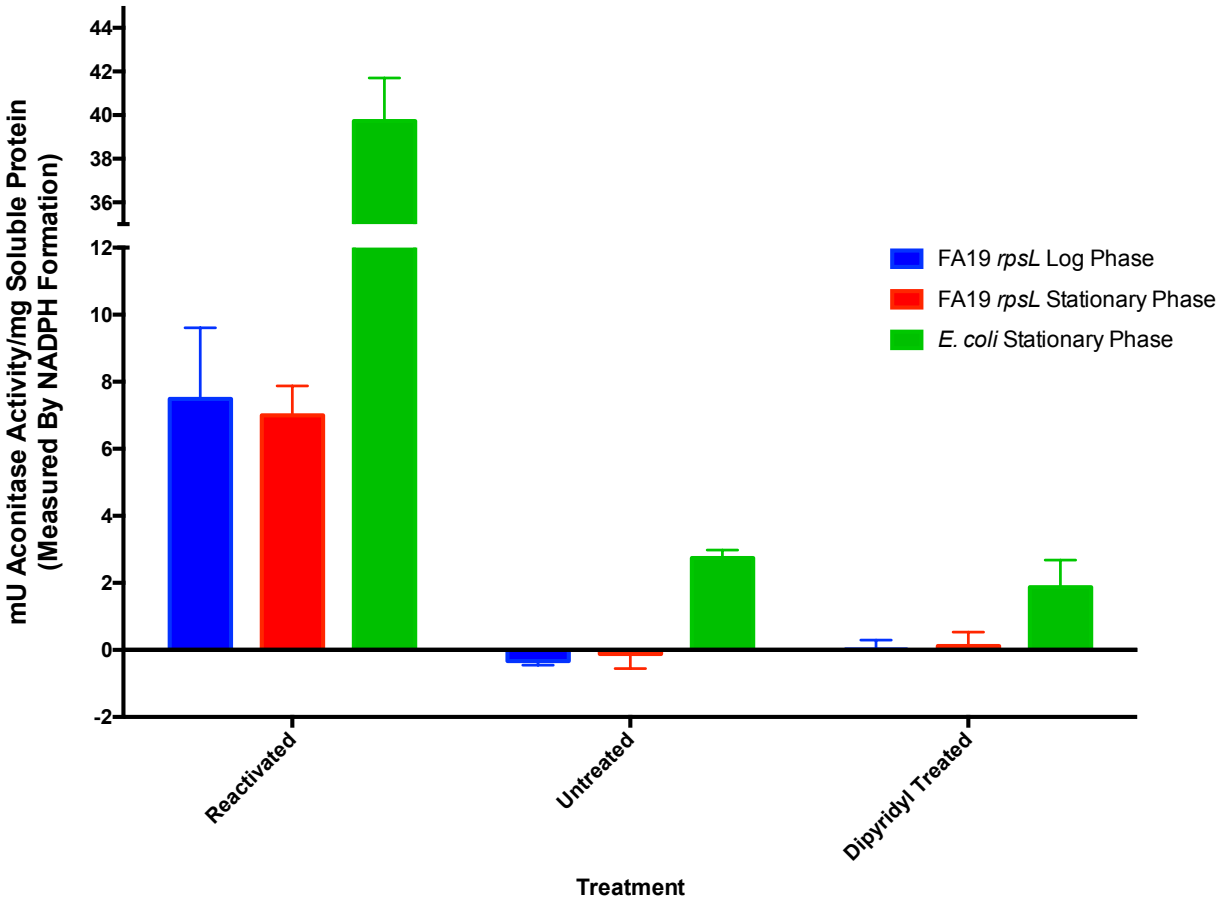

Figure 11

Aconitase activity per mg of soluble protein present in different preparations of cell lysates. One unit of aconitase activity is defined as the formation of one µmole of NADPH per minute as calculated using the coupled aconitase assay and absorbance of NADPH at 340nm.

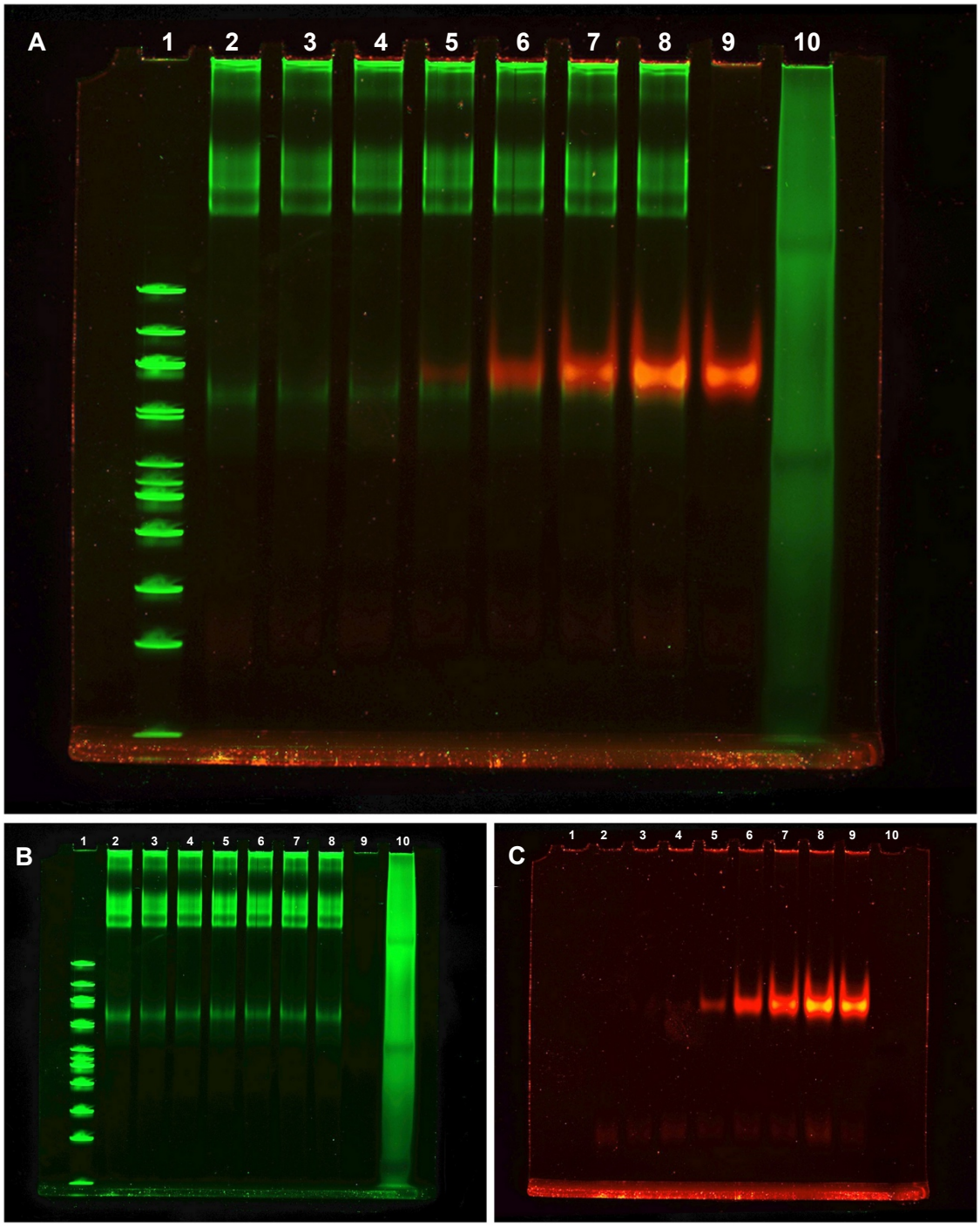

Figure 12
EMSA of *N. gonorrhoeae acnB* mRNA 5'UTR and Apo-AcnB protein. Lane 1 and 10 are dsDNA standards and a Page Ruler Plus Prestained protein ladder, respectively. Lanes 2-8 have 70ng *acnB* 5'UTR RNA. Lanes 3-8 have increasing amounts of Apo-AcnB protein starting with 25ng and doubling every lane to 800ng protein in lane 8. Lane 9 has only Apo-AcnB protein (800ng). The fainter lower protein band in lanes 2-9 is the RNase inhibitor. (A) Overlay of nucleic acid stain (B) and protein stain (C).

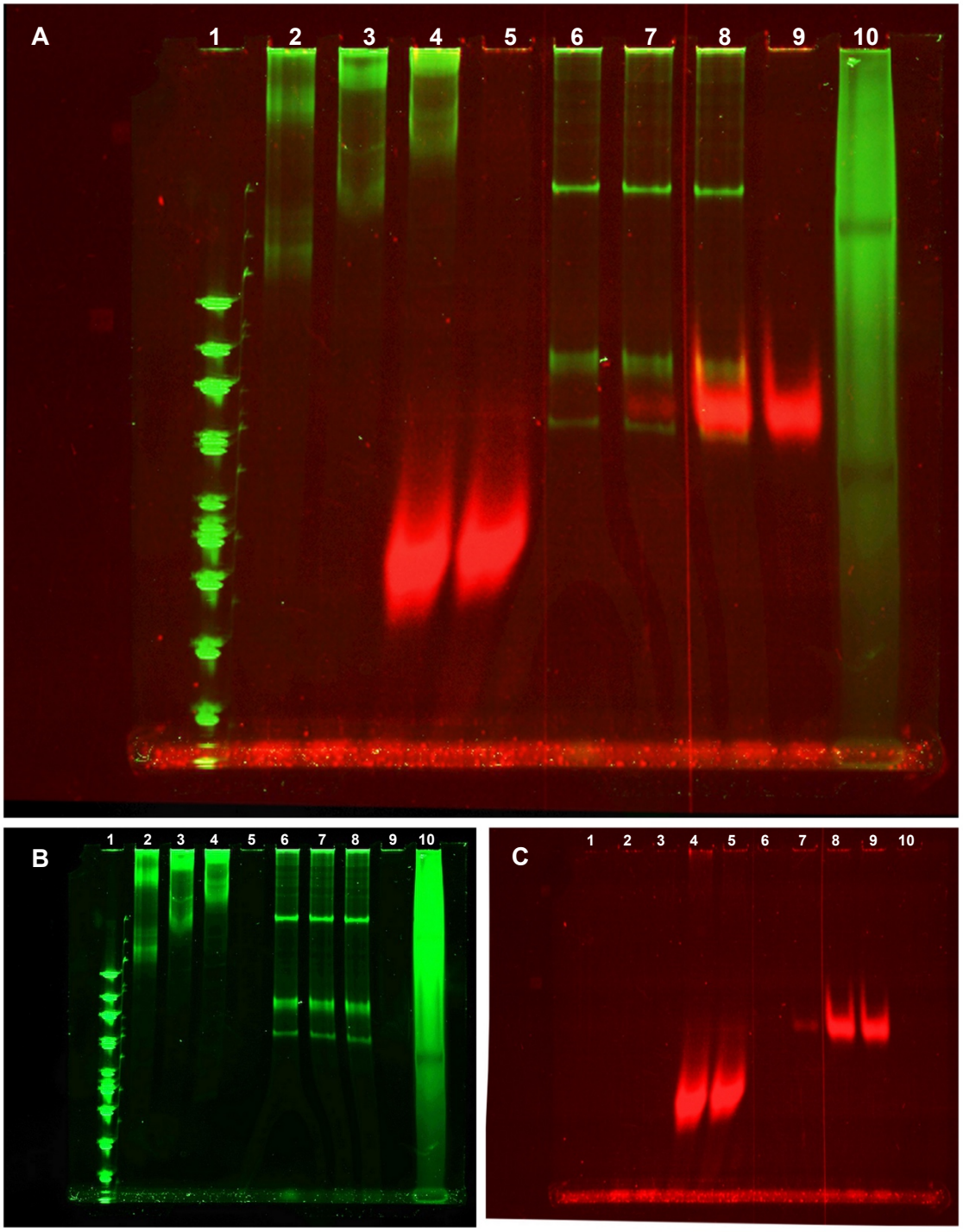

Figure 13

EMSA of *N. gonorrhoeae acnB* mRNA extended 3'UTR with Apo-AcnB protein and the positive control from *P. aeruginosa* (*tssa1* RNA and RsmA protein). Lane 1 and 10 are dsDNA standards and a Page Ruler Plus Prestained protein ladder, respectively. Lane 2: 70ng *tssa1* RNA only. Lane 3: 70 ng *tssa1* RNA and 100 ng RsmA. Lane 4: 70ng *tssa1* RNA and 800 ng RsmA. Lane 5: 800ng RsmA protein only. Lane 6: 70ng *acnB* extended 3'UTR RNA only. Lane 7: 70ng *acnB* extended 3'UTR RNA and 100ng Apo-AcnB protein. Lane 8: 70ng *acnB* extended 3'UTR RNA and 800ng Apo-AcnB protein. Lane 9: 800ng Apo-AcnB protein only. (A) Overlay of nucleic acid stain (B) and protein stain (C). The misshapen lane 5 is thought to be from a bubble in the electrophoresis apparatus.

Table 1

Oligos used for the amplification of segments of 16S rRNA and *acnB* mRNA in qPCR

Oligo Name	Sequence
5’ 16S 1325	GTGCATGAAGTCGGAATCGC
3’ 16S 1451	GCGGTTACCCTACCTACTTCTG
5’ *acnB* 1340	CTGCCTATCCGAAACCTGTCG
3’ *acnB* 1491	GCCGCCTGTACCGACTGTATC